Pharmaceutical Research, Vol. 26, No. 7, July 2009 (© 2009)
DOI: 10.1007/s11095-009-9875-5

Research Paper

PLGA and PHBV Microsphere Formulations and Solid-State Characterization: Possible Implications for Local Delivery of Fusidic Acid for the Treatment and Prevention of Orthopaedic Infections

Chiming Yang,[1] David Plackett,[2] David Needham,[3] and Helen M. Burt[1,4]

Received September 23, 2008; accepted March 16, 2009; published online April 21, 2009

Purpose. To develop and characterize the solid-state properties of poly(DL-lactic-co-glycolic acid) (PLGA) and poly(3-hydroxybutyric acid-*co*-3-hydroxyvaleric acid) (PHBV) microspheres for the localized and controlled release of fusidic acid (FA).
Methods. The effects of FA loading and polymer composition on the mean diameter, encapsulation efficiency and FA released from the microspheres were determined. The solid-state and phase separation properties of the microspheres were characterized using DSC, XRPD, Raman spectroscopy, SEM, laser confocal and real time recording of single microspheres formation.
Results. Above a loading of 1% (*w*/*w*) FA phase separated from PLGA polymer and formed distinct spherical FA-rich amorphous microdomains throughout the PLGA microsphere. For FA-loaded PLGA microspheres, encapsulation efficiency and cumulative release increased with initial drug loading. Similarly, cumulative release from FA-loaded PHBV microspheres was increased by FA loading. After the initial burst release, FA was released from PLGA microspheres much slower compared to PHBV microspheres.
Conclusions. A unique phase separation phenomenon of FA in PLGA but not in PHBV polymers was observed, driven by coalescence of liquid microdroplets of a DCM-FA-rich phase in the forming microsphere.

KEY WORDS: antibiotics; controlled drug delivery; fusidic acid; PLGA and PHBV microspheres; solid-state phase separation.

INTRODUCTION

Orthopaedic surgeries are routinely performed to restore structure and function to millions of people disabled by accidents and diseases. But even with modern day sterilization, aseptic surgical procedures and ultra-clean operation rooms, orthopaedic surgeries can still be complicated by infections (1). Thus, the treatments (2–5) and prevention (6–9) of orthopaedic infections have utilized prolonged systemic antibiotic therapy. However, serious problems can arise from this approach, including a failure to produce therapeutic tissue concentrations of the antibiotics because of relatively low vascularity within necrotic bone and implant in prosthetic joint infections. Local delivery of antibiotics offers significant advantages in the management and prevention of orthopaedic infections (10), and in this paper, we characterize the solid-state phase behavior of poly(DL-lactic-*co*-glycolic acid) (PLGA) and poly(hydroxybutyrate-*co*-hydroxyvalerate) (PHBV) microsphere formulations that could potentially improve local delivery of fusidic acid for the treatment and prevention of orthopaedic infections.

By direct application of antibiotics to the site of infection or potential infection, it is possible to achieve higher tissue levels and for a longer period of time, while simultaneously avoiding systemic side effects. These high local levels of directly applied antibiotics facilitate delivery by diffusion to avascular areas of the wound that are inaccessible by systemic antibiotics, which often can only be delivered in concentrations that may result in resistance (11).

The primary methods of local antibiotic delivery in orthopaedic surgeries over the past three decades, have been with antibiotic-loaded poly(methylmethacrylate) (PMMA)

Electronic supplementary material The online version of this article (doi:10.1007/s11095-009-9875-5) contains supplementary material, which is available to authorized users.

[1] Faculty of Pharmaceutical Sciences, The University of British Columbia, 2146 East Mall, Vancouver, B.C. V6T 1Z3, Canada.
[2] Risø National Laboratory for Sustainable Energy, Technical University of Denmark—DTU, Building 124, Frederiksborgvej 399, P.O. Box 49, DK-4000 Roskilde, Denmark.
[3] Department of Mechanical Engineering and Material Science, Duke University, Science Drive, Durham, North Carolina 27708, USA.
[4] To whom correspondence should be addressed. (e-mail: burt@interchange.ubc.ca)

ABBREVIATIONS: BSEM, Backscattering SEM; DSC, Differential scanning calorimetry; FA, Fusidic acid; HV, Hydroxyvaleric acid; PHBV, Poly(3-hydroxybutyric acid-*co*-3-hydroxyvaleric acid); PLGA, Poly(DL-lactic-co-glycolic acid); PLLA, Poly(L -lactic acid); PMMA, Poly(methylmethacrylate); SEM, Scanning electron microscopy; T_g, Glass transition temperature; T_m, Melting temperature; T_r, Enthalpy relaxation temperature; XRPD, X-ray powder diffraction; ΔH_m, Enthalpy of melting; ΔH_r, Enthalpy relaxation.

bone cement and beads (11–13). Nonetheless, there are disadvantages associated with PMMA carriers. PMMA is not biodegradable and not bioreabsorable, therefore it must be surgically removed from the implantation site following drug release. However, more importantly from a materials and performance standpoint, PMMA carriers provide a significantly sub-optimal antibiotic elution profile since the vast majority of the loaded antibiotic is retained in the matrix and not released (14–17). Due to the fundamental problems with PMMA, various biodegradable and bioresorbable carriers of antibiotics for the treatment and prevention of prosthetic joint infections have been studied based on poly (α-hydroxy acid) polymers such as PLGA (18–20) and PHBV (21–23). In particular, PLGA (19,20,24–26) and PHBV (27,28) microspheres have been used to deliver a variety of antibiotics for the treatment of bone infections.

With the increasing incidence of methicillin-resistant *S. aureus* (MRSA) and *S. epidermidis* found in orthopaedic infections, it has become a challenge to find efficacious treatments and preventions even with today's arsenal of antibiotics. Fusidic acid (FA) has been available since the 1960s (29) and is most active against *S. aureus*, *S. epidermidis*, and coagulase-negative staphylococci including strains that are methicillin-resistant that commonly cause prosthetic joint infections (3,29). However, systemic delivery of FA can lead to many serious toxicities (29–32). Although localized and controlled delivery of FA has been proposed, to date, only a limited number of studies, which include FA delivery via non-biodegradable PMMA bone cement (2,33,34), bioresorbable plaster of Paris (calcium sulphate hemihydrate) beads (35–37), and sodium fusidate (sodium salt of FA) from PLGA microspheres (38) have been documented in the literature.

In this work, we investigated the development and characterization of FA-loaded PLGA and PHBV microspheres for localized and controlled delivery. We have shown that encapsulation of FA in PLGA (but not PHBV) microspheres resulted in an interesting phase separation phenomenon of FA-rich spherical domains throughout the microsphere matrix and surface. From real time recordings of single microdroplets produced and positioned using micromanipulation video microscopy, this was attributed to a phase separation and coalescence of liquid phase FA-rich microdroplets produced within the microsphere during solvent evaporation and their exclusion from the phase-separated PLGA matrix upon hardening.

MATERIALS AND METHODS

Chemicals

FA (Mw 516.709 g/mol), PHBV (12 wt.% hydroxyvaleric acid, HV), poly(vinyl alcohol) (PVA, 98% hydrolyzed, Mw 13–23 g/mol), gelatin (type A, from porcine skin, bloom~300), dichloromethane (DCM), acetonitrile (ACN), chloroform, methanol, phosphoric acid, and the different reagents needed to prepare phosphate buffered saline (PBS, pH 7.4) solution were all obtained from Sigma-Aldrich (Oakville, ON, CA). PLGA (85/15 lactic acid/glycolic acid) with an intrinsic viscosity of 0.61 dL/g in chloroform (equivalent to *M*w ~86,000 g/mol) was obtained from Birmingham Polymers Inc. (Birmingham, AL, USA) and PLGA (50/50) with intrinsic viscosity of 0.58 dL/g in hexafluoroisopropanol (equivalent to Mw~84,000 g/mol) was obtained from Lactel® Absorbable Polymers (Pelham, AL, USA). Poly(L -lactic acid) (PLLA, Mw 100,000 g/mol) was obtained from Polysciences Inc (Warrington, PA, USA).

Fabrication of FA-Loaded PLGA and PHBV Microspheres

FA-loaded microspheres were synthesized by the oil-in-water (O/W) single emulsion solvent evaporation method as previously described (39). Three different initial drug loading, 10%, 20% and 30% (*w*/*w*) of FA relative to polymer were investigated. Varying amounts of FA and PLGA (85/15) were dissolved in 5 mL of DCM at a concentration of 10% (*w*/*v*) (40–42). For example, for 10% (*w*/*w*) FA loading, 45.45 mg of FA and 454.55 mg of PLGA were dissolved in 5 mL of DCM to obtain a 10% (*w*/*v*) solution. The FA and PLGA solution was then added drop-wise into 100 mL of 2.5% (*w*/*v*) PVA solution with an overhead propeller stirring at 600 rpm to form the O/W emulsion. The resulting emulsion was stirred continuously for 2.5 h at room temperature under the fume hood to evaporate the organic solvent. The FA-loaded PLGA microspheres were collected by centrifuging at 3,000 rpm for 5 min and subsequently washed four times with distilled water to remove residual DCM and PVA. The microspheres were then vacuum dried at room temperature and stored in a desiccator for further analysis. Residual DCM was not measured in the final microsphere products of this study. However, using similar processing conditions, Gangrade *et al.* have shown there was no detectable amount of residual DCM in the microspheres (43,44). FA-loaded PHBV microspheres were fabricated using the same procedures described above. To examine the effects of different polymers on the microsphere morphologies, 30% (*w*/*w*) FA-loaded PLGA (50/50) and PLLA microspheres were fabricated in the same manner as described above. In addition, the effects of using a different emulsifying agent in the aqueous solution on the morphology of microspheres of 30% (*w*/*w*) FA-loaded PLGA (85/15) were studied using gelatin instead of PVA (44).

Casting of FA and PLGA Films

Films containing varying weight % of FA and PLGA (85/15) were solution cast at a concentration of 10% (*w*/*v*) on Teflon® templates applied to glass slides. FA and PLGA were dissolved in DCM and the weight % of FA to PLGA (*w*/*w*) solutions were: 0.1%, 0.5%, 1%, 2%, 10%, 20%, 30%, 80%, 90%, 98%, 99%, 99.5% and 99.9% (*w*/*w*) FA.

Microsphere Particle Size Determination

FA-loaded PLGA and PHBV microspheres mean particle size and size distributions were determined using a Malvern Mastersizer 2000 (Malvern Inc., Malvern, Worcestershire, UK), laser diffraction particle size analyzer. Briefly, accurately measured (~5–10 mg) amount of microspheres were suspended in 5 mL of distilled water with two drops of 1% polysorbate 80 (Tween 80) and sonicated for 2 min to prevent aggregation of microspheres.

FA Encapsulation Efficiency

To determine FA encapsulation efficiency in the microsphere formulations, 5 mg of microspheres were dissolved in 1 mL of ACN or chloroform, and then 5 mL of PBS (pH 7.4) was added to precipitate the polymer. Subsequently, the sample was centrifuged at 3000 rpm for 5 min to spin down the precipitated polymer. The organic phase of the solution (ACN or chloroform) was further filtered with 0.45 μm PTFE syringe filter prior to HPLC (Waters® Millennium System) analysis that utilized a mobile phase of 50/30/20 (v/v/v) ACN/methanol/0.01 M phosphoric acid solution, flowing at 1 ml/min through a C_{18} reverse phase Novapak column (Waters®), with a 20 μl sample injection volume, and detection λ at 235 nm. FA content was quantified against a standard curve prepared by dissolving FA in ACN over a range of 0.01 to 1.0 mg/mL.

In Vitro FA Release from PLGA and PHBV Microspheres

In vitro FA release from PLGA and PHBV microsphere formulations was carried out in PBS (pH 7.4) at 37°C. For release studies, 5 mg of FA-loaded microspheres were placed into 15 mL of PBS and the samples were tumbled end-over-end at 10 rpm in a thermostatically controlled oven at 37°C. At specified time points, the sample tubes were centrifuged at 3,000 rpm for 5 min, 5 mL of samples were then withdrawn for HPLC analysis to determine the amount of drug released. The remaining medium was removed and replaced with fresh PBS (pH 7.4) to maintain sink conditions. Concentrations of FA in the release medium were measured directly using the above HPLC method.

Scanning Electron Microscope (SEM), Backscattering SEM (BSEM), and Laser Confocal Microscope Analyses

The morphologies and structures of the FA-loaded microsphere formulations and cast films were characterized using a combination of SEM, BSEM, and 3-D laser confocal microscope. For conventional SEM analysis, samples were sputter-coated with a layer of 60:40 alloy of gold:palladium using a Denton Vacuum Desk II sputter-coater (Moorestown, NJ) at 50 mTorr. SEM images were then captured using a Hitachi S-3000N system (Tokyo, Japan) scanning at 10–20 keV. To avoid obscuring the fine detailed surface characteristics of the FA-loaded PLGA and PHBV microspheres, uncoated samples were analyzed using either a Hitachi S-4700 Field Emission Scanning Electron Microscope (FESEM, Tokyo, Japan) operated at 1 keV to produce BSEM micrographs or a Keyence VK-9700 3-D laser confocal microscope that employed two light sources: a short waveform laser light and a white light source to produce laser confocal images.

Raman Spectroscopy

High spatial resolution Raman spectroscopy surface mapping analyses of FA-loaded PLGA and PHBV microsphere formulations were kindly performed by Dr. Tim Smith of Renishaw, plc (Wotton-under-Edge, UK). Specifically, Raman spectra were obtained on a Renishaw RM100 confocal Raman Microscope (Renishaw, plc), recorded at a spatial resolution of 1–3 μm on a 62–157 μm×69–163 μm image area producing up to 3968 Raman mapped spectra as the laser scanned the analysis area. Images were subsequently created using component method (using FA and polymer reference spectra) and coloured images were generated from StreamLine™ images of Anadin Extra tablet as reference with argon ion laser excitation at λ_0=785 nm.

X-ray Powder Diffraction (XRPD)

XRPD patterns of FA and FA-loaded PLGA and PHBV microsphere formulations were acquired using a Bruker D8 Advance (Madison, WI) diffractometer in Bragg-Brentano configuration with a Cu source at 25°C. Samples were scanned from 2–50° 2θ, using a step size of 0.020°, and a step time of 1 second per step. Approximately 200–300 mg of sample was packed onto a standard Bruker sample holder with sample spinning during data acquisition to avoid preferential orientation of sample.

Differential Scanning Calorimetry (DSC)

DSC analysis of the FA-loaded PLGA and PHBV microspheres was performed on a TA Instruments DSC Q100 (New Castle, DE, USA) with liquid nitrogen cooling system. Accurately weighed samples (~2–5 mg) were hermetically sealed in aluminum pan and heated from 25°C to 250°C at a rate of 10°C/min under nitrogen flow. The initial heat scan was followed by a rapid quench cooling scan from 250°C to −80°C at a rate of 35°C/min and then a second heating scan from −80°C to 250°C at a rate of 10°C/min. For FA-loaded PLGA microspheres, the peak temperature of the first endothermic transition in the first heating cycle was recorded as the temperature at which enthalpy relaxation occurred (T_r), while glass transition temperature (T_g) was taken as the midpoint of the heat capacity change in the second heating to be clearly distinguishable from the enthalpy relaxation. Since PHBV does not possess an enthalpy relaxation, T_g was taken as the midpoint of the heat capacity change in the first heating cycle for FA-loaded PHBV microspheres. In addition, the double endothermic transitions (melt-recrystallization-remelting) of PHBV (45) were recorded in the first heating cycle.

Micromanipulation and Video Imaging of Microsphere Formation

Real-time recordings of the formation of single FA-loaded PLGA microspheres were captured for the 30% (*w*/*w*) FA-loaded PLGA (85/15) microspheres. Briefly, drug and polymer solution in DCM was formed at the tip of a 5 μm diameter borosilicate glass micropipett, in a solution of 0.01 M SDS solution contained in a customized design glass chamber placed under a conventional inverted light microscope with ×60 oil immersion objective, connected to a CCD camera, monitor and video recorder (46). Once a single droplet of the drug and polymer solution was formed at the tip of the micropipette, it was held there by gentle suction pressure, allowing the DCM to "evaporate", (i.e. to dissolve from the droplet into the aqueous phase), as it would in the normal bulk-suspension microsphere fabrication process.

Control PLGA and FA-loaded PHBV microsphere formation and their solidification processes were similarly video imaged as above.

RESULTS

FA-Loaded PLGA and PHBV Microspheres

To investigate FA-loaded PLGA (85/15) and PHBV microsphere formulations, three different initial drug loading, 10%, 20% and 30% (*w*/*w*) were used and the resulting encapsulation efficiency and mean diameter of the microsphere were determined. Increasing the initial drug loading from 10–30% (*w*/*w*) in the PLGA (85/15) microspheres produced a corresponding increase in encapsulation efficiency from 76±6% to 89±1% (n=6), with no significant changes in the mean diameter, 92±10 to 114±4 μm (n=6), respectively. The encapsulation efficiency and mean diameter of FA-loaded PHBV were not affected by initial drug loading and they were approximately 100±7% and 138±6 μm, respectively.

Surface Characterization Studies

SEM analyses revealed the detailed surface morphologies of the FA-loaded PLGA (85/15) and PHBV microspheres (Fig. 1). All FA-loaded PLGA (85/15) microspheres showed spherical and relatively uniform protrusions (bumps) on their surfaces regardless of the changes in the initial drug loading. The only difference observed was the increase in size and height of the protrusion on the surfaces with an increase in initial FA loading in the PLGA (85/15) microspheres (Fig. 1B–D). The surfaces of control (no drug) PLGA (85/15) microspheres were smooth (Fig. 1A). Moreover, microspheres fabricated at 30% (*w*/*w*) FA loading using different PLGA (50/50) (Fig. 2A) and PLLA (Fig. 2B) polymers, as well as 30% (*w*/*w*) FA-loaded PLGA (85/15) microspheres prepared using gelatin as a different emulsifying agent (Fig. 2C) also possessed spherical protrusions on their surfaces.

FA-loaded PHBV microspheres surface morphologies were also affected by initial FA loading, and were quite different in appearance to FA-loaded PLGA and PLLA microspheres, with recessed spherical dimples on the surfaces that increase as initial drug loading increased (Fig. 1J–L). The surfaces of control (no drug) PHBV microspheres were relatively smooth (Fig. 1I), although not as smooth as pure PLGA (85/15) microspheres (Fig. 1A).

Fine surface morphological details of the FA-loaded PLGA (85/15) and PHBV microspheres were obtained with the use of laser confocal and BSEM analyses where there are no requirements for a coating layer and are shown in Fig. 3. The spherical protrusions on the PLGA microsphere surfaces appeared to possess distinct boundaries (Fig. 3A and B). In addition, the spherical microdomains were found throughout the entire PLGA (85/15) matrix as demonstrated in BSEM micrograph of the microsphere cross-section in Fig. 3C, although these inclusions were not as large as the ones at the surface. BSEM images of FA-loaded PHBV microspheres (Fig. 3D), revealed cracked, rough and pitted surfaces not observed with conventional SEM.

Phase Separation of FA in PLGA Microspheres

The existence of phase separated regions in the FA-loaded PLGA (85/15) microspheres was confirmed and identified chemically by Raman spectroscopy surface mapping analyses (Fig. 4A–D). The PLGA polymer-rich regions (Fig. 4B, shown in green), and FA-rich regions (Fig. 4C, shown in red) could be clearly identified, and upon merging of the two images, it was evident that the spherical protrusions were FA-rich microdroplet phase distributed throughout the PLGA-rich matrix of the microsphere (Fig. 4D). SEM images of 10, 20 and 30% (*w*/*w*) FA-loaded PLGA (85/15) microspheres before and after 7 days of drug release in PBS (pH 7.4) shown in Fig. 1F–H, also support the Raman findings that the spherical protrusions on the surfaces of the microspheres were primarily composed of FA, since the protrusions were eliminated following 7 days of drug release (i.e. the protruded FA microdomains have dissolved off and formed depressions on the surface).

Real-time video images of a single FA-loaded PLGA microsphere are illustrated in Fig. 5 (shown as time separated screen captures, with the full length video available online as *Electronic Supplementary Material*), and demonstrate the phase separation process on the surface and within the interior of the forming microsphere (for scale, screen height is ~25 μm). As DCM solvent evaporates from the initial ~40 μm microsphere droplet (Fig. 5A, time=0 s), the overall size of the microsphere droplet begins to decrease (Fig. 5B, time=3 s). Further DCM evaporation leads to numerous phase-separated FA liquid microdroplets being formed throughout the microsphere (Fig. 5C, time=5 s) and shortly after, there was evidence of excessive coalescence of these FA liquid phase microdroplets (Fig. 5D, time=8 s) to form larger phase-separated FA-rich microdomains (Fig. 5E, time=9 s) that are clearly visible within the bulk and also on the surface of the microsphere as spherical protrusions at the end of the solidification process (Fig. 5F, time=13 s).

Raman spectroscopy surface mapping of the FA-loaded PHBV microsphere (Fig. 4E), showed that the PHBV polymer (Fig. 4F, illustrated in green), and FA drug (Fig. 4G, illustrated in red) were both distributed uniformly throughout the entire microsphere with no apparent phase separation of FA from the polymer matrix. Real-time video recordings were also made of single FA-loaded PHBV microspheres showing no phase separation of FA consistent with the Raman spectroscopy mapping (data not shown). Moreover, after 7 days of drug release there was no significant changes in the surface morphologies of the FA-loaded PHBV microspheres (Fig. 1N-P). The SEM images of the PHBV microspheres only showed the accumulation of salts on the surfaces from the PBS solution after drying for analyses.

Miscibility and Phase Separation of FA and PLGA in Solvent-Cast Films

We evaluated FA and PLGA (85/15) miscibility characteristics and the phase separation phenomenon in cast films where drug loading can be completely and accurately controlled. It was shown that the miscibility limit for FA in PLGA (85/15) was approximately 1% (*w*/*w*) (Fig. 6A). At FA

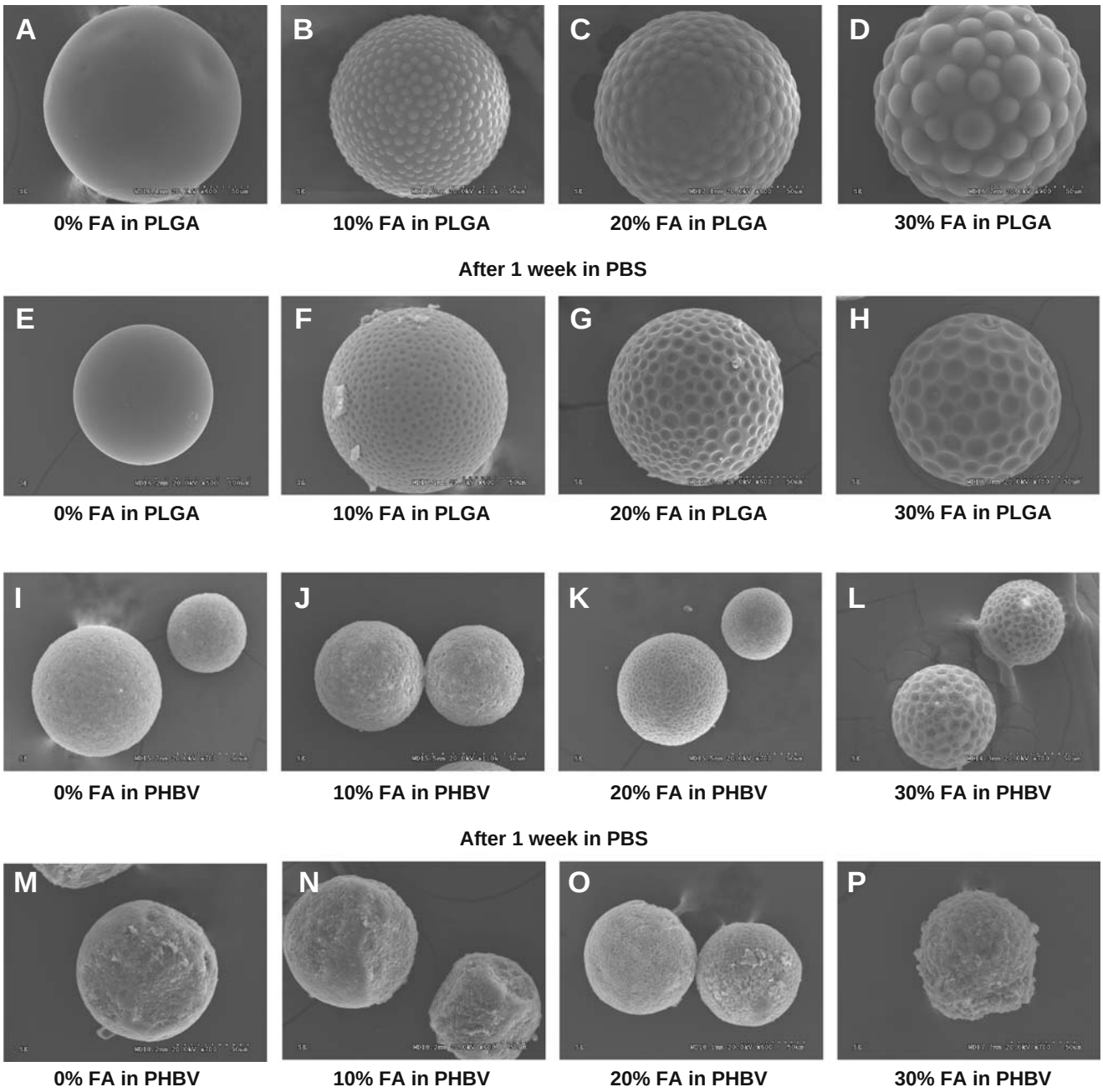

Fig. 1. SEM micrographs illustrating the effects of different drug loading on FA loaded PLGA (85/15) microsphere surface morphologies (*A–D*) and the changes after 7 days of drug release (*E–H*). Also shown are the effects of different drug loading on FA loaded PHBV (12% HV) microsphere surface morphologies (*I–L*) and the change after 7 days of drug release (*M–P*). In cases where different magnifications were used, *scale bar above magnification* provides a reference for comparison between micrographs.

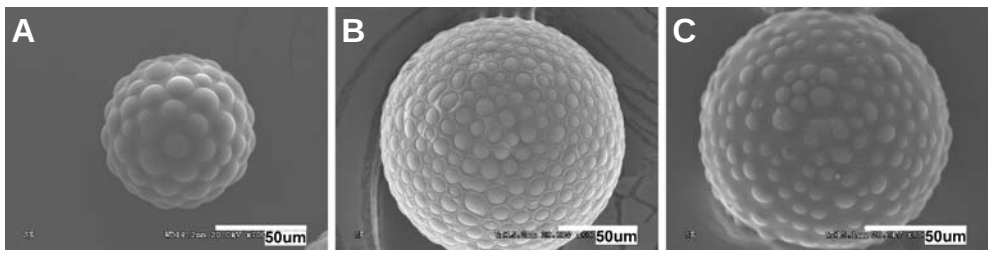

Fig. 2. SEM micrographs illustrating the effects of different polymers and emulsifying agent on 30% (*w*/*w*) FA-loaded microsphere surface morphologies. *A* PLGA (50/50) using PVA as emulsifying agent, *B* PLLA using PVA as emulsifying agent, and *C* PLGA (85/15) using gelatin as emulsifying agent.

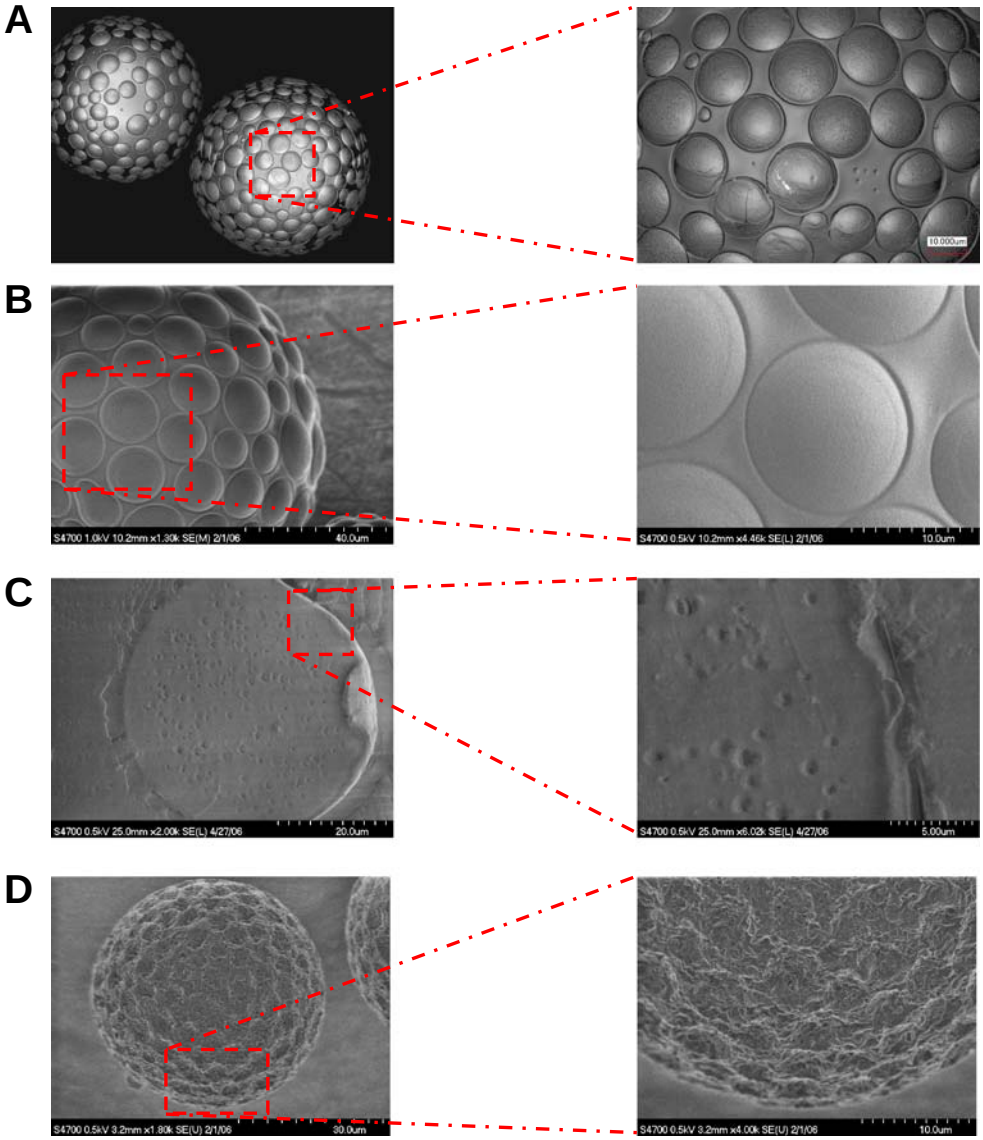

Fig. 3. Detailed surface and interior morphologies of 30% FA loaded PLGA (85/15) and PHBV (12% HV) microspheres. *A* Laser confocal microscope images of PLGA microsphere, *B* BSEM micrographs of PLGA microsphere, *C* BSEM micrographs of sectioned PLGA microsphere, and *D* BSEM images of PHBV microsphere. In cases where different magnifications were used, scale bar above magnification provides a reference for comparison between micrographs.

loading of 2% (*w*/*w*) and above, the films were phase-separated (Fig. 6B). At 30% (*w*/*w*) FA loading, the distinctive spherical microdomains were evidently formed within the PLGA matrix (Fig. 6C). At the other extreme of the two component phase diagram, even at very low concentration (0.1% *w*/*w*) PLGA (85/15) was not miscible in FA and the two components were completely phase separated (data not shown).

XRPD Characterization of FA-Loaded PLGA and PHBV Microspheres

To determine whether phase separated, FA-rich microdomains were crystalline in nature, XRPD was carried out and results are shown in Fig. 7. Even at the highest drug loading of 30% (w/w) FA in the PLGA microspheres, there was no evidence of crystallinity in the sample, illustrated by the characteristic amorphous halo in the XRPD diffraction pattern (Fig. 7B). All other FA-loaded PLGA and PLLA microspheres and all FA-loaded PHBV microspheres produced a similar amorphous x-ray pattern.

Thermal Analysis of FA-Loaded PLGA and PHBV Microspheres

DSC scans of FA-loaded PLGA microspheres showed an enthalpy relaxation endotherm (Fig. 8A) and T_g for PLGA at ~46–50°C (Fig. 8B), and a T_g for FA at ~117–118°C (Fig. 8A) for higher FA loadings. The DSC result of the pure FA drug in the amorphous state illustrating the T_g is shown in Fig. 8D.

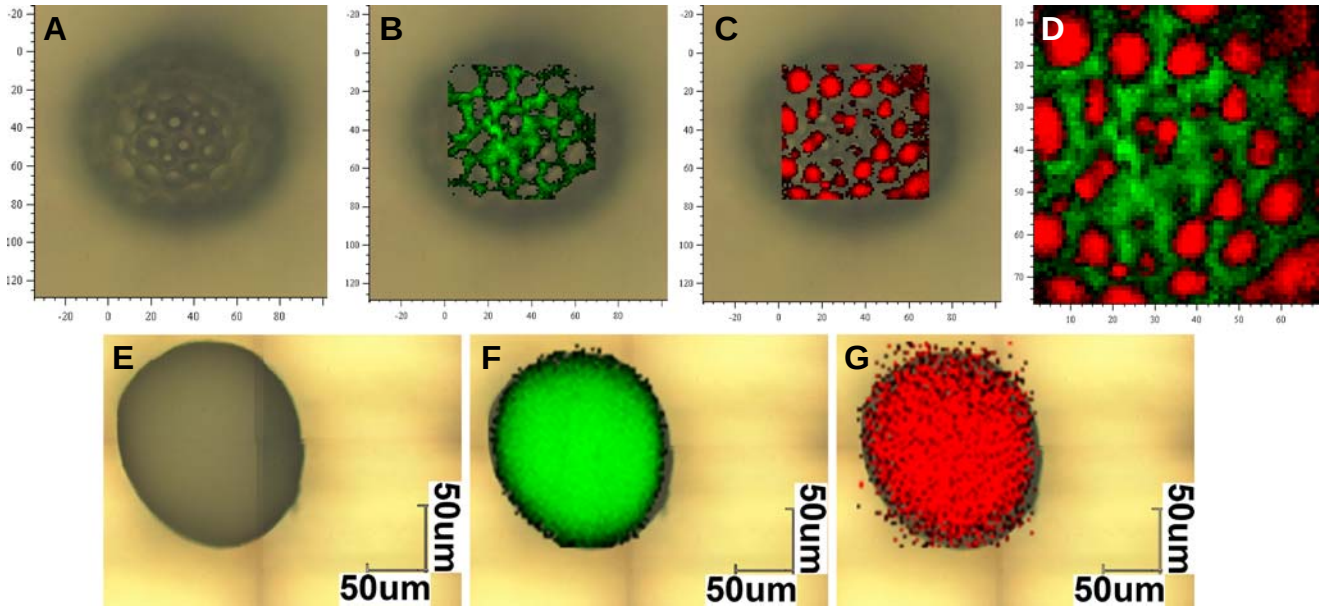

Fig. 4. Raman spectroscopy images of FA distribution in 30% FA loaded PLGA (85/15) and PHBV (12% HV) microspheres. PLGA microsphere images include: *A* White light microsphere montage, ×50 magnification, *B* distribution of PLGA-rich regions (green) across microsphere, *C* distribution of FA-rich regions (*red*) across microsphere, and *D* combined distribution of the two regions across microsphere. PHBV microsphere images include: *E* White light microsphere montage, ×20 magnification, *F* distribution of PHBV (green) across microsphere, and *G* distribution of FA (*red*) across microsphere.

DSC analyses of FA-loaded PHBV microspheres revealed a T_g for PHBV around 57–59°C and double melting peaks in the range of 133–152°C corresponding to PHBV's melting-recrystallization-remelting process upon heating (Fig. 8C). All the thermal events are summarized in Table I. The presence of FA was found to increase the enthalpy relaxation temperature, T_r and the T_g of PLGA. Whereas in FA-loaded PHBV microspheres, the presence of FA had no effect on T_g, but decreased the melting, T_{m1} and remelting, T_{m2} of PHBV polymer (Table I).

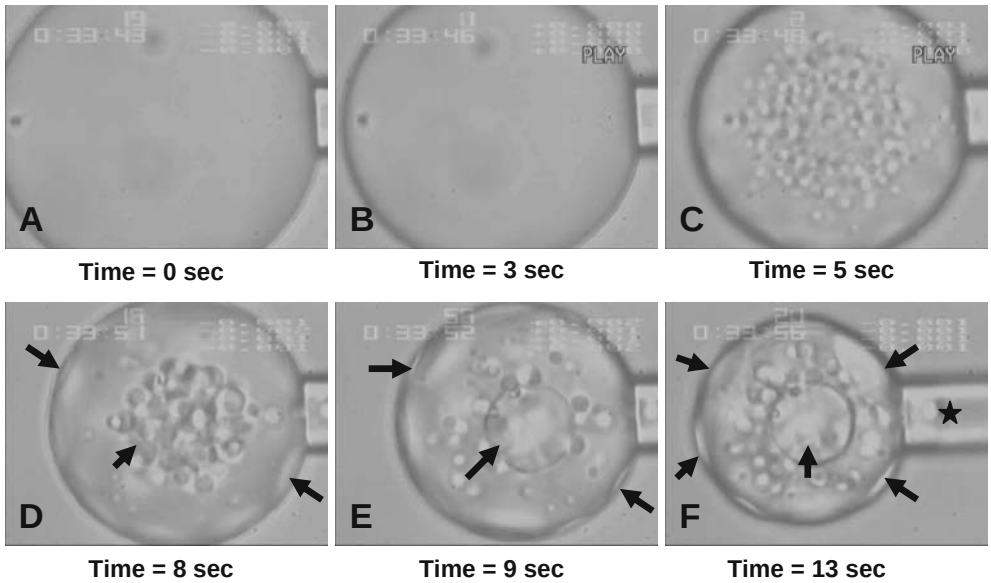

Fig. 5. Time lapsed video images illustrating the formation of a single 30% FA loaded PLGA (85/15) microsphere with an initial polymer and drug concentration of 10% (*w/v*). The initial FA/PLGA/DCM droplet was blown from a micropipette into 0.01 M SDS aqueous solution at room temperature. *Arrows* illustrate the phase separated FA-rich microdomains, while *star* indicates the micropipette. For scale, screen height is ~25 μm. The full video showing the FA phase separation phenomenon and microsphere solidification process can be view online at the URL xxx. *A* Time=0 s, *B* Time=3 s, *C* Time=5 s, *D* Time=8 s, *E* Time=9 s, *F* Time=13 s.

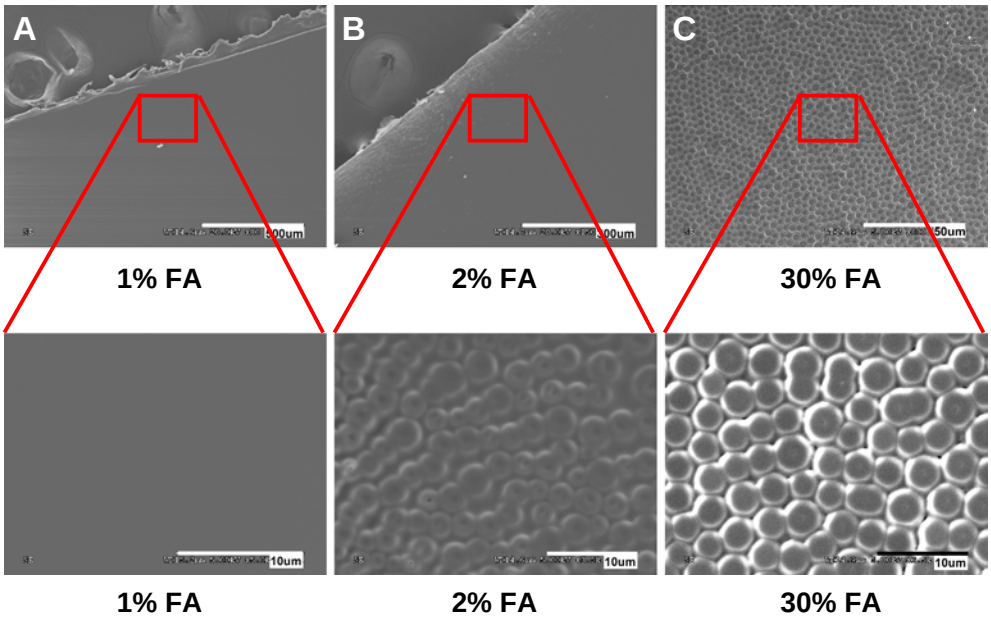

Fig. 6. SEM micrographs of % *w/w* FA in PLGA (85/15) films solvent-cast from DCM illustrating the miscibility characteristics of FA and PLGA. In cases where different magnifications were used, *scale bar above magnification* provides a reference for comparison between micrographs.

Drug Release Profiles of FA-Loaded PLGA and PHBV Microspheres

FA-loaded PLGA (85/15) and PHBV microsphere drug release profiles were determined in PBS (pH 7.4) and are shown in Fig. 9. Overall, cumulative release of FA from all PLGA and PHBV microspheres demonstrated similar biphasic release profiles with a rapid burst phase followed by a phase of slow controlled release over 21 days. The increase in FA loading from 10% to 30% (*w/w*) produced a larger burst phase of release, leading to higher overall FA released.

DISCUSSION

Fabrication of microspheres using solvent evaporation is a variable and complex process with many adjustable parameters (39, 47, 48). Nevertheless, in the end though, it should obey the laws of material phase behavior. In this study, the effects of initial drug loading were investigated for the formulation of FA-loaded PLGA and PHBV microspheres. For FA-loaded PLGA (85/15) microspheres, increasing the initial drug loading produced a corresponding increase in encapsulation efficiency because at higher FA loading, the external aqueous phase was more likely to be saturated with

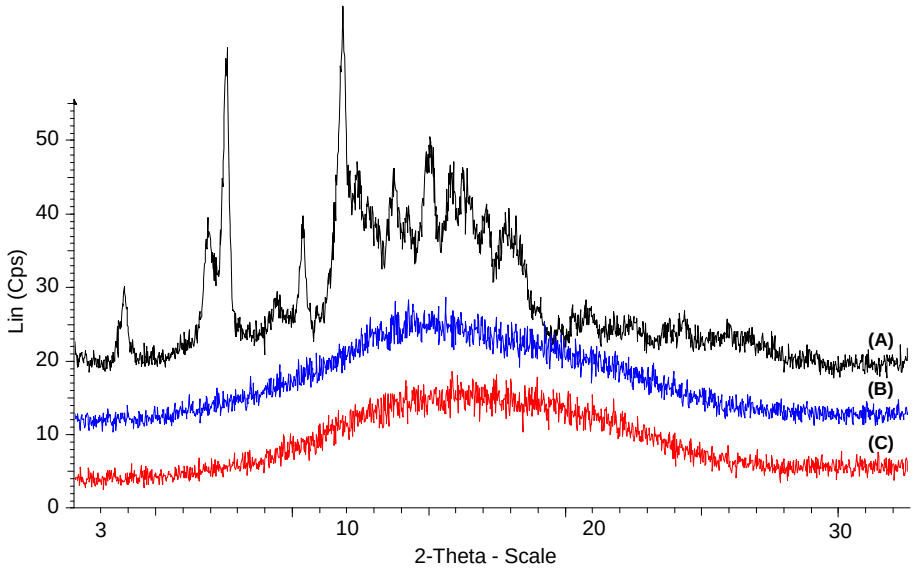

Fig 7. XRPD patterns of solid-state *A* FA as received, *B* 30% (*w/w*) FA loaded PLGA (85/15) microspheres, and *C* control (no drug) PLGA (85/15) microspheres.

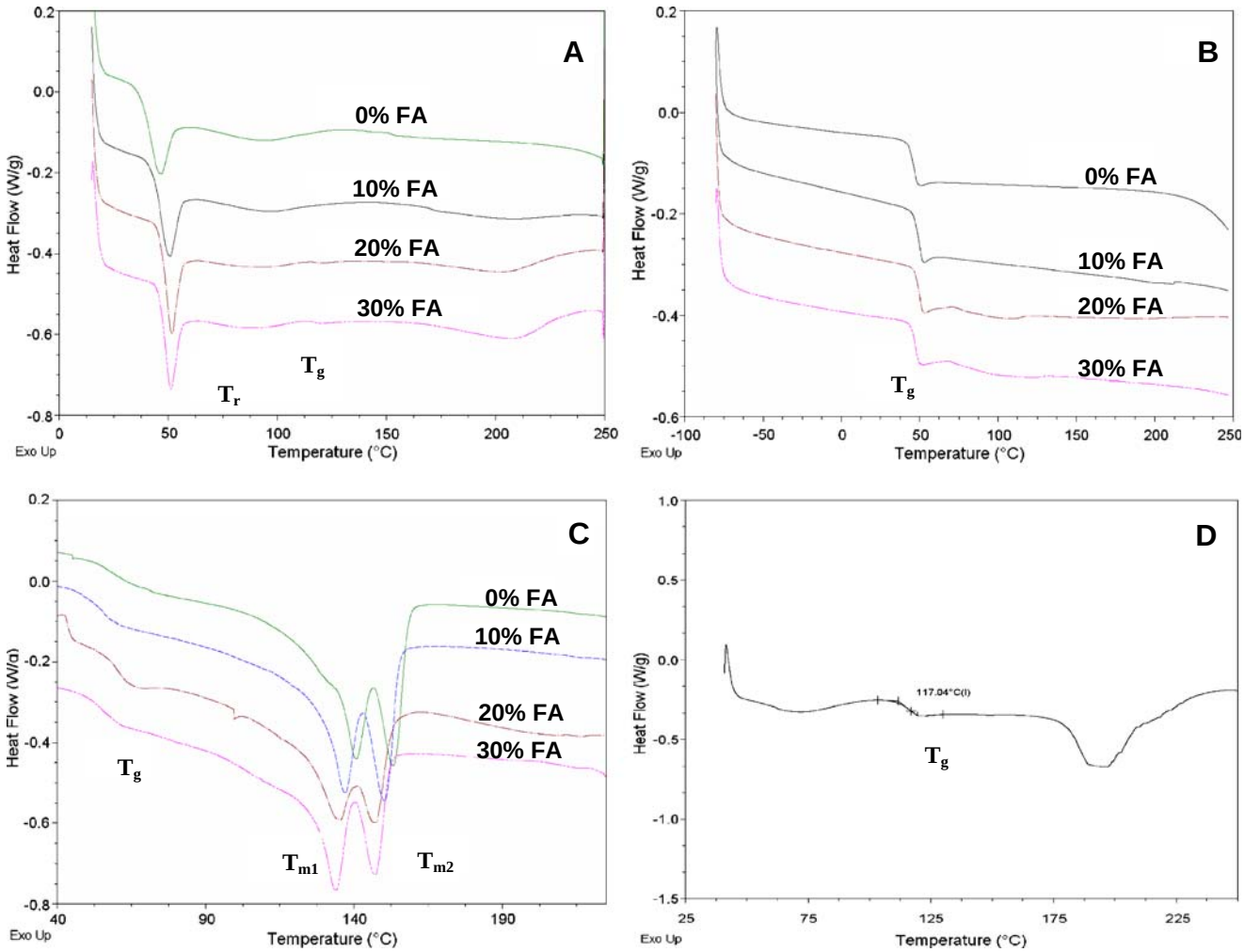

Fig. 8. DSC thermograms of *A* first heating cycle of FA loaded PLGA (85/15) microspheres illustrating the enthalpy relaxation temperature, T_r, of the PLGA polymer and the glass transition temperature, T_g of FA, *B* second heating cycle (after quench cooled) of FA loaded PLGA (85/15) microspheres showing the T_g of the PLGA polymer, *C* FA loaded PHBV (12% HV) microspheres illustrating the T_g and double melting temperature, T_{m1} and T_{m2} of the PHBV polymer, and *D* pure amorphous FA illustrating the T_g of the drug.

FA (FA solubility in aqueous phase, pH 5.7 was determined to be ~50 μg/mL), thus reducing the diffusion and partition of FA into the external aqueous phase, and allowing more FA to be entrapped in the microsphere.

A combination of SEM, BSEM, laser confocal microscope, Raman spectroscopy analysis and miscibility determination with solvent-cast films all support the observation that FA phase separates from PLGA polymers. Phase separation of FA occurred in all PLGA compositions (i.e. 50/50, 85/15, 100/0) and changes in initial drug loading (data not shown). Gangrade *et al.* found that changing the emulsifying agents (PVA to gelatin) significantly altered the microspheres properties (44). However, in our study, changing the emulsifying agent from PVA to gelatin in the external aqueous phase during the fabrication process did not affect the phase separation of FA from PLGA. Increasing FA loadings from 10% to 30% (*w*/*w*) greatly exceeded the miscibility of FA in PLGA (~1%) and produced larger FA-rich phase separated microdomains that may also contain small amounts of PLGA chain segments and residual DCM and water solvent.

The separated FA-rich phase was present throughout the PLGA matrix illustrated by microsphere sections and seen by real-time video recordings of single microspheres during their formation. The representative video images of the FA-loaded PLGA microsphere showed that the formation of FA-rich microdomains was driven by the coalescence of highly concentrated FA microdroplets within the liquid phase PLGA microsphere prior to final hardening. As the DCM solvent "evaporates", FA-rich microdroplets (resolution is about 1 μm) begin to phase separate out and continued DCM evaporation leads to decreases in the overall microsphere size. The video clearly shows individual FA-rich microdroplets coalescing together until larger and stable microdroplets are formed throughout the solidified microsphere. Interestingly, in the final stages of solidification when most of the solvent has "evaporated", these phase-separated FA-rich domains are seen to appear and grow at the interface, and soon form rounded protrusions as seen in the video (and SEM) images. It's as though they are indeed being physically excluded from the solidifying PLGA rich matrix. Similarly, the FA phase separation and coalescence phenomena were seen in video recordings for the different FA loadings (10% and 20%) in PLGA. They were not however, observed with FA-loaded PHBV microspheres, and were not present in

Table 1. Summary of the Thermal Properties of FA and FA Loaded PLGA (85/15) and PHBV (12% HV) Microspheres Obtained Using DSC, $n=3$

Formulations	Polymer transitions								Fusidic acid transitions	
	T_r (°C)[a]	ΔH_r (J/g)[b]	T_g (°C)[c]	ΔC_p J/(g C)	T_{m1} (°C)[d]	ΔH_{m1} (J/g)[e]	T_{m2} (°C)[f]	ΔH_{m2} (J/g)[g]	T_g (°C)	ΔC_p J/(g °C)
0% FA loaded PLGA	46.6±0.6	8.79±0.54	45.9±1.2	0.51±0.6	–	–	–	–	–	–
10% FA loaded PLGA	50.1±0.3	8.86±0.36	49.9±0.1	0.53±0.03	–	–	–	–	–	–
20% FA loaded PLGA	50.9±0.9	8.25±0.39	49.6±1.1	0.52±0.03	–	–	–	–	118.4±0.2	0.02±0.01
30% FA loaded PLGA	51.0±0.3	7.75±0.11	48.1±0.7	0.49±0.02	–	–	–	–	116.8±0.7	0.03±0.01
0% FA loaded PHBV	–	–	59.0±1.6	0.31±0.09	139.78±0.88	9.63±3.34	152.77±0.73	8.50±1.17	–	–
10% FA loaded PHBV	–	–	57.2±0.8	0.49±0.08	136.41±0.88	13.20±1.99	150.10±0.86	10.35±1.15	–	–
20% FA loaded PHBV	–	–	57.1±2.1	0.44±0.05	133.77±0.75	4.91±0.47	147.27±0.52	2.26±1.36	–	–
30% FA loaded PHBV	–	–	57.3±2.0	0.45±0.07	134.07±0.20	12.93±2.71	147.24±0.33	8.96±1.62	–	–

[a] T_r enthalpy relaxation temperature. The peak temperature of the first endothermic transition in the first heating cycle
[b] ΔH_r enthalpy relaxation. The first endothermic transition in the first heating cycle
[c] T_g glass transition temperature. The midpoint of the heat capacity change in the second heating cycle for FA-loaded PLGA microspheres and first heating cycle for FA-loaded PHBV microspheres.
[d] T_{m1} first melting temperature. The peak temperature of the first endothermic transition in the first heating cycle
[e] ΔH_{m1} enthalpy of melting. The first endothermic transition in the first heating cycle
[f] T_{m2} remelting temperature after recrystallization. The peak temperature of the second endothermic transition in the first heating cycle
[g] ΔH_{m2} enthalpy of melting after recrystallization. The second endothermic transition in the first heating cycle

control (no drug) PLGA microspheres (data not shown). Panyam *et al.* (49) have previously observed phase separation of hydrophobic drug from PLGA and PLLA, and suggested the result was due to the different solid-state solubility of the drug in the polymers, while Vasanthavada *et al.* (50,51) also investigated the mechanism and kinetics of phase separation of small molecules in polymer as a result of solid-state solubility. However, in both the Panyam *et al.* and Vasanthavada *et al.* studies, no distinctive spherical microdomains of the phase separated drug were observed. The phase separated FA-rich spherical microdomains observed throughout the PLGA matrix in this study resemble the formation of microdomains in composite (blended) polymer microspheres, where the microdomains were the results of non-equilibrium of two phase separated polymers (52). In any event, the most striking observation from the real-time video recordings of single microspheres is that the FA-rich phase, that must still contain some DCM solvent, is liquid, and so is subject to the same effects of interfacial tension, forming minimum interfacial areas and subject to coalescence if such liquid domains touch in the shrinking liquid PLGA-DCM microsphere.

Interestingly, FA was not phase separated when formulated in PHBV, which is another polymer in the family of poly

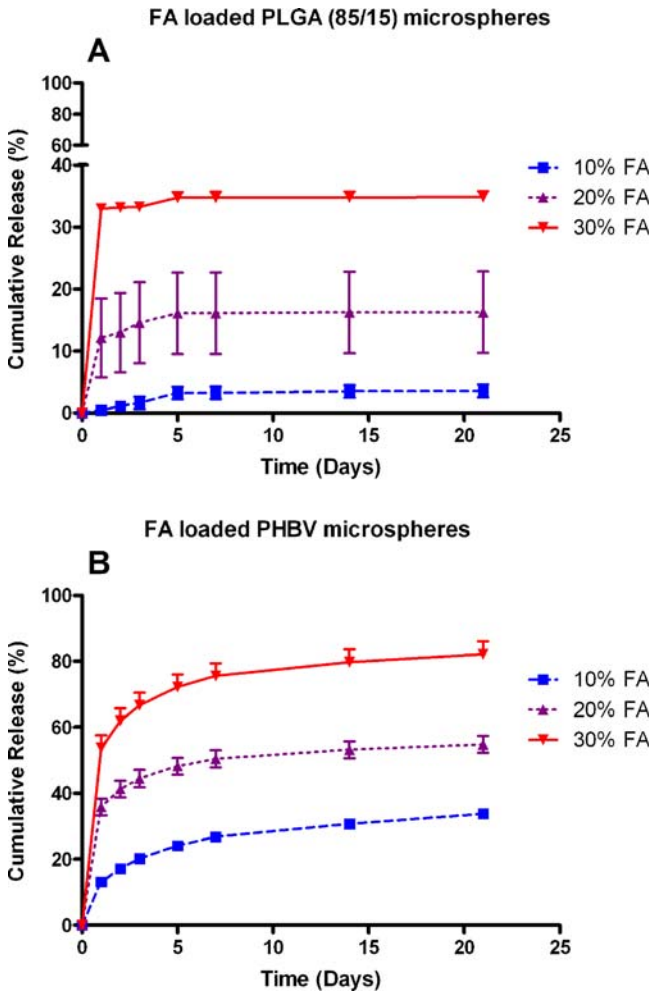

Fig. 9. *In vitro* FA release profiles from *A* PLGA (85/15) and *B* PHBV microsphere formulations performed in PBS (pH 7.4) at 37°C, $n=3$.

(α-hydroxy acid) polymers like PLGA and PLLA since FA was found to be distributed uniformly over the microsphere surface. The subtle differences in molecular structure of the polymer chain such as the extra methyl group found in the backbone of the repeat units of PHBV compared to PLGA/PLLA polymer could be a possible explanation for FA to not be phase separated from the PHBV matrix. The extra methyl group might contribute to PHBV being more hydrophobic than PLGA/PLLA, thus allowing FA, a hydrophobic drug, to have greater solid-state miscibility with PHBV.

The FA-rich solid microdomains phase separated out in the microsphere were found to be amorphous due to the lack of crystallinity peaks in the XRPD patterns, and absence of a melt endotherm and presence of a T_g in the DSC thermograms at high FA loadings (Fig. 8A). The inability of FA to recrystallize even at 30% (*w*/*w*) FA loading could be attributed to multiple factors as follows: the constant mechanically agitated solvent evaporation process; possible presence of residual solvents (both DCM and water); presence of a very small amount of dispersed PLGA (i.e. below 0.1% *w*/*w*), and even the kinetics required for recrystallization. The absence of crystalline drug in PLGA particle formulations has also been reported for other hydrophobic drugs that phase separated from the polymer matrix (49,53).

An FA melting event (175°C) was not detected for all drug loadings. At higher FA loadings (20% and 30%), DSC analyses showed a T_g of FA at ~116–118°C and this was consistent with the XRPD analyses showing that the phase separated FA microdomains in PLGA microspheres were in the amorphous state. Enthalpy relaxation events were observed at the T_g of the PLGA microspheres in the first heating cycle of the DSC scans (Fig. 8A). Similar to the T_g, enthalpy relaxation is due to short range order that arises in the glassy phase of a polymer matrix and short range order may arise within the matrix during the microsphere formation process (40). The miscible amount of FA within the PLGA matrix of the FA-loaded microspheres may as well have acted as an anti-plasticizing agent reducing the molecular mobility (or free volume) of the PLGA as shown by the increase in both the T_r and T_g (54,55). Since up to a maximum of 1% FA was miscible in the PLGA matrix, all the FA-loaded microspheres produced the same increase in enthalpy relaxation, T_r and T_g (Table I). An increase in T_r and T_g were similarly observed for other reported PLGA and PLLA microsphere formulations in which the added PVA surfactant (56), and paclitaxel drug (42), respectively, acted as anti-plasticizers.

On the contrary, for the FA-loaded PHBV microspheres, the uniformly distributed, (and presumably single phase) FA within the solid-state polymer matrix had no (statistically significant) effect on the T_g (~57–59°C), but behaved as a plasticizer and lowered the melt temperature, T_{m1} (~140°C), and remelt temperature, T_{m2} (~152°C) of PHBV (45). Additional evidence supporting the single phase solid solution form of FA in PHBV, the DSC analysis was unable to record any T_g for FA even at 30% loading (Fig. 8C).

The burst phase of the biphasic release profiles of all FA-loaded PLGA microsphere formulations was likely a result of the dissolution of the phase separated FA located on the surface (Fig. 1B–D). Increasing FA loading produced a larger burst release due to the increased amount of FA phase separated on the surface as shown in Fig. 1B to D as larger surface protrusions. The subsequent release after the initial burst phase was very slow for all the PLGA microsphere formulations and this was controlled by the slow diffusional release of FA through the polymer matrix as well as the slow degradation of PLGA (85/15) that occurs at ~15–20 weeks (57, 58). The remaining unreleased FA was found entrapped within the PLGA microspheres when analyzed after the release study (data not shown). FA-loaded PHBV microsphere formulations also showed a significant burst release due to FA being distributed on the surfaces, with increased FA loading producing a larger burst. The subsequent continuous release of FA from PHBV microspheres compared to the very slow release from PLGA microspheres might have resulted from the cracked, rough, and possibly porous microsphere surfaces of the PHBV microspheres.

CONCLUSION

In the process of formulating FA in PLGA, PLLA and PHBV microspheres, we observed an interesting phase separation phenomenon of FA in PLGA and PLLA but not in PHBV polymer. It was found that FA was miscible in solid solution in the PLGA polymer matrix up to a maximum of 1% and was well integrated with the PLGA polymer chains, as demonstrated by the increase in T_r and T_g. Above 1%, though, liquid microdroplets of FA phase separated from the PLGA matrix during DCM solvent removal and, driven by a coalescence behavior of these liquid DCM-FA-rich domains, formed distinct, large, completely amorphous, spherical FA-rich solid microdomains throughout the microsphere, but especially excluded to the microsphere interface. The biphasic drug release profiles were relatively well defined with an initial burst release for all FA-loaded PLGA and PHBV microsphere formulations. The amount of drug released in this initial burst phase was controlled to some extent by the initial FA loading. Thus, the findings of this study provide a better understanding of the solid-state characteristics of FA in PLGA, PLLA and PHBV microspheres that will influence the design of local delivery system for FA.

ACKNOWLEDGMENTS

We would like to thank Dr. Tim Smith and Renishaw plc, Wotton-under-Edge, UK for his assistance and the use of the confocal Raman microscope. We also like to thank John Jackson, Kevin Letchford, Sam Gilchrist and Ben Wasserman for their excellent technical assistance and discussion. This work was supported by Canadian Institutes of Health Research (CIHR) New Emerging Team (NET) Grant. In addition, the authors would like to thank Natural Sciences and Engineering Council of Canada (NSERC) for financial support to C.Y. in the form of a NSERC Postgraduate Scholarship-Doctoral (PGS-D).

REFERENCES

1. Trampuzand A, Widmer AF. Infections associated with orthopedic implants. Curr Opin Infect Dis 2006;19:349–56.

2. Atkinsand B, Gottlieb T. Fusidic acid in bone and joint infections. Int J Antimicrob Agents 1999;12:S79–93. doi:10.1016/S0924-8579(98)00077-6.
3. Darleyand AP, MacGowan ESR. Antibiotic treatment of Gram-positive bone and joint infections. J Antimicrob Chemother 2004;53:928–35. doi:10.1093/jac/dkh191.
4. Segreti J, Trenholme GM, Nelson JA. Prolonged suppressive antibiotic therapy for infected orthopaedic prostheses. Clin Infect Dis 1998;27:711–3. doi:10.1086/514951.
5. Tattevin P, Cremieux AC, Pottier P, *et al*. Prosthetic joint infection: when can prosthesis salvage be considered? Clin Infect Dis 1999;2:292–5. doi:10.1086/520202.
6. Bengtson S, Borgquist L, Lindgren L. Cost analysis of prophylaxis with antibiotics to prevent infected knee arthroplasty. Br Med J 1989;299:719–20.
7. Hill C, Flamant R, Mazas F, Evrard J. Prophylactic cefazolin *versus* placebo in total hip replacement. Report of a multicentre double-blind randomised trail. Lancet 1981;1:795–6. doi:10.1016/S0140-6736(81)92678-7.
8. Periti P, Mini E, Mosconi G. Antimicrobial prophylaxis in orthopedic surgery: the role of teicoplanin. J Antimicrob Chemother 1998;41:329–40. doi:10.1093/jac/41.3.329.
9. Periti P, Stringa G, Mini E. Comparative multicenter trail of teicoplanin *versus* cefazolin for antimicrobial prophylaxis in prosthetic joint implant surgery. Italian study group for antimicrobial prophylaxis in orthopedic surgery. Eur J Clin Microbiol Infect Dis 1999;18:119. doi:10.1007/s100960050238.
10. Rauschmann MA, Wichelhaus TA, Stirnal V, Dingeldein E, Zichner L, Schnettler R, Alt V. Nanocrystalline hydroxyapatite and calcium sulphate as biodegradable composite carrier material for local delivery of antibiotics in bone infections. Biomaterials 2005;26:2677–84. doi:10.1016/j.biomaterials.2004.06.045.
11. Hassenand MJ, Spangehl AD. Practical applications of antibiotic-loaded bone cement for treatment of infected joint replacements. Clin Orthop Relat Res 2004;427:79–85.
12. Adams K, Couch L, Cierny G, Calhoun J, Mader JT. *In vitro* and *in vivo* evaluation of antibiotic diffusion from antibiotic-impregnated polymethylmethacrylate beads. Clin Orthop 1992;278:244–52.
13. Kanellakopoulouand K, Giamarellos-Bourboulis EJ. Carrier systems for the local delivery of antibiotics in bone infections. Drugs 2000;59:1223–32. doi:10.2165/00003495-200059060-00003.
14. Hoff SF, Fitzgerald Jr RH, *et al*. The depot administration of penicillin G and gentamicin acrylic bone cement. J Bone Jt Surg 1981;63:798–804.
15. Holmand NJ, vejlsgaard R. The *in vitro* elution of gentamicin sulphate from methylmethacrylate bone cement-A comparative study. Acta Orthop Scand 1976;47:144–8.
16. Vogt S, Kuehn KD, Ege W, Pawlik K, Schnabelrauch M. Novel polylactide-based release systems for local antibiotic therapies. Materialwissenschaft und Werkstofftechnik 2003;34:1041–7. doi:10.1002/mawe.200300701.
17. Wahlig H, Dingeldein E, Bergmann R, Reuss K. The release of gentamicin from polymethylmethacrylate beads: an experimental and pharmacokinetics study. J Bone Jt Surg 1978;60:270.
18. Wang G, Liu SJ, Ueng SW-N, Chan EC. The release of cefazolin and gentamicin from biodegradable PLA/PGA beads. Int J Pharm 2004;273:203–12. doi:10.1016/j.ijpharm.2004.01.010.
19. Naraharisetti PK, Lew MDN, Fu YC, Lee DJ, Wang CH. Gentamicin-loaded discs and microspheres and their modifications: characterization and *in vitro* release. J Control Release 2005;102:345–59. doi:10.1016/j.jconrel.2004.10.016.
20. Yenice I, Calis S, Atilla B, Kas HS, Oezalp M, Ekizoglu M, Bilgili H, Hincal AA. *In vitro*/*in vivo* evaluation of the efficiency of teicoplanin-loaded biodegradable microparticles formulated for implantation to infected bone defects. J Microencapsul 2003;20:705–17. doi:10.1080/0265204031000154179.
21. Gursel I, Korkusuz F, Turesin F, Gurdal Alaeddinoglu N, Hasirci V. *In vivo* application of biodegradable controlled antibiotic release systems for the treatment of implant-related osteomyelitis. Biomaterials 2000;22:73–80. doi:10.1016/S0142-9612(00)00170-8.
22. Rossi S, Azghani AO, Omri A. Antimicrobial efficacy of a new antibiotic-loaded poly(hydroxybutyric-co-hydroxyvaleric acid) controlled release system. J Antimicrob Chemother 2004;54:1013–8. doi:10.1093/jac/dkh477.
23. Yagmurlu MF, Korkusuz F, Gursel I, Korkusuz P, Ors U, Hasirci V. Sulbactam-cefoperazone polyhydroxybutyrate-co-hydroxyvalerate (PHBV) local antibiotic delivery system: *in vivo* effectiveness and biocompatibility in the treatment of implant-related experimental osteomyelitis. J Biomed Materi Res 1999;46:494–503. doi:10.1002/(SICI)1097-4636(19990915)46:4<494::AID-JBM7>3.0.CO;2-E.
24. Jacob E, Cierny G, Fallon MT, McNeill JF, Siderys GS. Evaluation of biodegradable cefazolin sodium microspheres for the prevention of infection in rabbits with experimental open tibial fractures stabilized with internal fixation. J Orthop Res 1993;11:404–11. doi:10.1002/jor.1100110312.
25. Jacob E, Cierny G, Zorn K, McNeill JF, Fallon MT. Delayed local treatment of rabbit tibial fractures with biodegradable cefazolin microspheres. Clin Orthop Relat Res 1997;336:278–85. doi:10.1097/00003086-199703000-00036.
26. Jacob E, Setterstrom JA, Bach DE, Heath Iii JR, McNiesh LM. Cierny G. Evaluation of biodegradable ampicillin anhydrate microspheres for local treatment of experimental staphylococcal osteomyelitis. Clin Orthop Relat Res 1991;267:237–44.
27. Li H, Chang J. Preparation, characterization and *in vitro* release of gentamicin from PHBV/wollastonite composite microspheres. J Control Release 2005;107:463–73. doi:10.1016/j.jconrel.2005.05.019.
28. Sendil D, Gursel I, Wise DL, Hasirci V. Antibiotic release from biodegradable PHBV microparticles. J Control Release 1999;59:207–17. doi:10.1016/S0168-3659(98)00195-3.
29. Mandell LA, Mandell GL, Bennett JE, Dolin R. Fusidic Acid. Mandell, Douglas and Bennett's Principles and Practic of Infectious Diseases, Vol. 5, Churchill Livingstone, Philadelphia, 2000, p. 306.
30. Christiansen K. Fusidic acid adverse drug reactions. Int J Antimicrob Agents 1999;12(Suppl 2):S3–9. doi:10.1016/S0924-8579(98)00068-5.
31. Dollery C. Fusidic Acid. Therapeutic Drugs, Vol. 2, Churchill Livingstone, London, New York, Philadelphia, San Francisco, Sydney, Toronto, 1999, p. F177.
32. Turnidge J. Fusidic acid pharmacology, pharmacokinetics and pharmacodynamics. Int J Antimicrob Agents 1999;12:S23–34. doi:10.1016/S0924-8579(98)00071-5.
33. Andrews HJ, Arden GP, Hart GM, Owen JW. Deep infection after total hip replacement. J Bone Jt Surg 1981;63B:53–7.
34. Coombs RR, Menday AP. Fusidic acid in orthopaedic infections due to coaguluase-negative staphylococci. Curr Med Res Opin 1985;9:587–90.
35. Bouillet R, Bouillet B, Kadima N, Gillard J. Treatment of chronic osteomyelitis in Africa with plaster implants impregnated with antibiotics. Acta Orthop Belg 1989;55:1–11.
36. Mackey D, Varlet A, Debeaumont D. Antibiotic loaded plaster of paris pellets: an *in vitro* study of a possible method of local antibiotic therapy in bone infection. Clin Orthop and Relat Res 1982;167:263–8.
37. Mousset B, Benoit MA, Delloye C, Bouillet R, Gillard J. Biodegradable implants for potential use in bone infection. An *in vitro* study of antibiotic-loaded calcium sulphate. Int Orthop 1995;19:157–61. doi:10.1007/BF00181861.
38. Cevher E, Orhan Z, Sensoy D, Ahiskali R, Kan PL, Sagirli O, Mulazimoglu L. Sodium fusidate-poly(D,L-lactide-co-glycolide) microspheres: preparation, characterisation and *in vivo* evaluation of their effectiveness in the treatment of chronic osteomyelitis. J Microencapsul 2007;24:577–95. doi:10.1080/02652040701472584.
39. O'Donnell PB, McGinity JW. Preparation of microspheres by the solvent evaporation technique. Adv Drug Deliv Rev 1997;28:25–42. doi:10.1016/S0169-409X(97)00049-5.
40. Liggins RT, Burt HM. Paclitaxel loaded poly(L-lactic acid) microspheres: properties of microspheres made with low molecular weight polymers. Int J Pharm 2001;222:19–33. doi:10.1016/S0378-5173(01)00690-1.
41. Liggins RT, Burt HM. Paclitaxel loaded poly(l-lactic acid) (PLLA) microspheres II. The effect of processing parameters on microsphere morphology and drug release kinetics. Int J Pharm 2004;281:103–6. doi:10.1016/j.ijpharm.2004.05.027.
42. Liggins RT, Burt HM. Paclitaxel-loaded poly(L-lactic acid) microspheres 3: Blending low and high molecular weight

polymers to control morphology and drug release. Int J Pharm 2004;282:61–71. doi:10.1016/j.ijpharm.2004.05.026.
43. Gangrade N, Price JC. Simple gas chromatographic headspace analysis of residual organic solvent in microspheres. J Pharm Sci 1992;81:201–202. doi:10.1002/jps.2600810221.
44. Gangrade N, Price JC. Poly(hydroxybutyrate-hydroxyvalerate) microspheres containing progesterone: preparation, morphology and release properties. J Microencapsul 1991;8:185–202. doi:10.3109/02652049109071487.
45. Gunaratne LMWK, Shanks RA. Melting and thermal history of poly(hydroxybutyrate-co-hydroxyvalerate) using step-scan DSC. Thermochimica Acta 2005;430:183–90. doi:10.1016/j.tca.2005.01.060.
46. Duncan PB, Needham D. Microdroplet dissolution into a second-phase solvent using a micropipet technique: test of the Epstein-Plesset model for an aniline–water system. Langmuir 2006;22:4190–7. doi:10.1021/la053314e.
47. Freita A, Merkle HP, Gander B. Microencapsulation by solvent extraction/evaporation: reviewing the state of the art of microsphere preparation process technology. J Control Release 2005;102:313–32. doi:10.1016/j.jconrel.2004.10.015.
48. Mohamed F, van der Walle CF. Engineering biodegradable polyester particles with specific drug targeting and drug release properties. J Pharm Sci 2008;97:71–87. doi:10.1002/jps.21082.
49. Panyam J, Williams D, Dash A, Leslie-Pelecky D, Labhasetwar V. Solid-state solubility influences encapsulation and release of hydrophobic drugs from PLGA/PLA nanoparticles. J Pharm Sci 2004;93:1804–14. doi:10.1002/jps.20094.
50. Vasanthavada M, Tong WQ, Joshi Y, Kislalioglu MS. Phase behavior of amorphous molecular dispersions II: role of hydrogen bonding in solid solubility and phase separation kinetics. Pharm Res 2005;22:440–8. doi:10.1007/s11095-004-1882-y.
51. Vasanthavada M, Tong WQ, Joshi Y, Kislalioglu MS. Phase behavior of amorphous molecular dispersions I: determination of the degree and mechanism of solid solubility. Pharm Res 2004;21:1598–606. doi:10.1023/B:PHAM.0000041454.76342.0e.
52. Ma GH, Nagai M, Omi S. Study on preparation and morphology of uniform artificial polystyrene-poly(methyl methacrylate) composite microspheres by employing the spg (shirasu porous glass) membrane emulsification technique. J Colloid Interface Sci 1999;214:264–82. doi:10.1006/jcis.1999.6188.
53. Vega E, Gamisans F, Garcia ML, Chauvet A, Lacoulonche F, Egea MA. PLGA nanospheres for the ocular delivery of flurbiprofen: drug release and interactions. J Pharm Sci. 2008;97:1–12.
54. Garcia A, Iriarte M, Uriarte C, Iruin JJ, Etxeberria A, del Rio J. Antiplasticization of a polyamide: a positron annihilation lifetime spectroscopy study. Polymer 2004;45:2949–57. doi:10.1016/j.polymer.2004.02.045.
55. Slark AT. The effect of intermolecular forces on the glass transition of solute-polymer blends. Polymer 1997;38:2407–14. doi:10.1016/S0032-3861(96)00782-3.
56. Bouissou C, Rouse JJ, Price R, van der Walle CF. The influence of surfactant on PLGA microsphere glass transition and water sorption: remodeling the surface morphology to attenuate the burst release. Pharm Res 2006;23:1295–305. doi:10.1007/s11095-006-0180-2.
57. Anderson JM, Shive MS. Biodegradation and biocompatibility of PLA and PLGA microspheres. Adv Drug Deliv Rev 1997;28:5–24. doi:10.1016/S0169-409X(97)00048-3.
58. Miller RA, Brady JM, Cutright DE. Degradation rates of oral resorbable implants (polylactates and polyglycolates): rate modification with changes in PLA/PGA copolymer ratios. J Biomed Materi Res 1977;11:711–9. doi:10.1002/jbm.820110507.